[4]M. Kastner, Phys. Rev. Letters 28, 355 (1972).

[5]A preliminary report was presented by M. Kastner [Bull. Am. Phys. Soc. 17, 345 (1972)].

[6]We appreciate the generosity of J. Wagner of Servo Corporation of America in furnishing samples of As_2S_3.

[7]W. C. Schneider and K. Vedam, J. Opt. Soc. Am. 60, 800 (1970).

[8]We thank J. de Neufville and D. Sarrach of Energy Conversion Devices, Inc. for preparing samples.

[9]Our results for As_2S_3 are in agreement with those of R. K. Galkiewicz and J. Tauc, Solid State Commun. (to be published).

[10]K. Vedam, E. D. D. Schmidt, and R. Roy, J. Am. Ceramic Soc. 49, 531 (1966); K. Vedam and T. A. Davis, J. Opt. Soc. Am. 57, 1140 (1967).

[11]D. F. Gibbs and G. J. Hill, Phil. Mag. 9, 367 (1964).

[12]G. A. N. Connell and W. Paul, J. Non-Cryst. Solids 8–10, 215 (1972); D. L. Camphausen, G. A. N. Connell, and W. Paul, Phys. Rev. Letters 26, 184 (1971).

[13]Note that since K is always positive, $(1/n)(dn/dP)$ is positive even if $(1/nl)/[d(nl)/dP]=0$ [see Eq. (3)].

[14]Connell and Paul used the K values of the corresponding crystal in extracting $(1/n)/(dn/dP)$ from $(1/nl)/[d(nl)/dP]$ for the amorphous tetrahedral semiconductors. The fact that $(1/n)/(dn/dP)$ determined in this way is the same for the amorphous and crystalline phases of Ge, GaAs, and GaP means that $(1/nl)/[d(nl)/dP]$ is the same for the two phases. Furthermore, it would be fortuitous to arrive at the same $(1/n)/(dn/dP)$ if the K were not in fact the same for the two phases.

[15]J. Tauc, A. Abraham, L. Pajasova, R. Grigorovici, and A. Vancu, in *Proceedings of the Conference on the Physics of Non-Crystalline Solids, Delft*, 1964, edited by J. A. Prins (North-Holland, Amsterdam, 1965), p. 606.

[16]J. Stuke, J. Non-Cryst. Solids 4, 1 (1970).

[17]E. Mohler, J. Stuke, and G. Zimmerer, Phys. Status Solidi 22, K49 (1967).

[18]A. G. Leiga, J. Appl. Phys. 39, 2149 (1968); J. Opt. Soc. Am. 58, 880 (1968); 58, 1441 (1968).

[19]In the ϵ_2 spectra of SiO_2, for example, there is little remnant of the two-peak structure. As ionicity increases, the $LP-\sigma^*$ and $\sigma-\sigma^*$ peaks become closer in energy. See H. Philipp, Solid State Commun. 4, 73 (1966).

[20]Van Vechten uses the Penn model: $n^2-1=(\hbar\omega_p/E_g)^2 \times(1-E_g/4E_F)$. Since $(1-E_g/4E_F)$ is close to unity, he neglects its pressure dependence, in which case Eq. (11) is obtained.

[21]J. C. Phillips, Phys. Rev. Letters 20, 550 (1968).

[22]For rhombic sulphur the values of n for different polarizations all fall within 0.1 of 2.15 [*American Institute of Physics Handbook*, 2nd ed. (McGraw-Hill, New York, 1963)].

[23]G. Lucovsky, A. Mooradian, W. Taylor, G. B. Wright, and R. C. Keezer, Solid State Commun. 5, 113 (1967).

[24]P. C. Taylor, S. G. Bishop, and D. L. Mitchell, Phys. Rev. Letters 27, 414 (1971); D. L. Mitchell, S. G. Bishop, and P. C. Taylor, J. Non-Cryst. Solids 8–10, 231 (1972).

[25]D. L. Dexter and W. R. Heller, Phys. Rev. 91, 273 (1953).

[26]P. Grosse, *Die Festkorpereigenschaften von Tellur* (Springer-Verlag, Berlin, 1969), Vol. 48.

[27]H. Krebs, *Fundamentals of Inorganic Crystal Chemistry* (McGraw-Hill, London, 1968).

[28]N. F. Mott and R. W. Gurny, *Electronic Processes in Ionic Crystals* (Oxford U. P., London, 1940).

[29]J. C. Phillips, *Covalent Bonding in Crystals, Molecules and Polymers* (University of Chicago Press, Chicago, 1970).

[30]H. Mueller, Phys. Rev. 47, 947 (1935).

PHYSICAL REVIEW B VOLUME 6, NUMBER 6 15 SEPTEMBER 1972

Theory of Photon-Drag Effect in Polar Crystals*

Jick H. Yee
Lawrence Livermore Laboratory, University of California, Livermore, California 94550
(Received 7 April 1972)

The theory of the photon-drag effect in polar crystals is considered using Fröhlich's model for the electron-phonon interaction. An equation is derived for the electric field generated by this effect. Numerical examples are given for CdS crystals.

I. INTRODUCTION

Recent advances in high-intensity laser technology have made it possible for us to observe many new and interesting phenomena in some semiconductors. Among these are the multiple-photon absorption process, harmonic generation, self-induced transparency, and photon-drag effect.[1–4] The photon-drag effect arises from the transfer of momentum from photons to the free carriers (either holes or electrons) through photon-electron-phonon interactions.[4,5] As a result of the transfer of momentum, a net flow of charge appears in the direction of propagation of the electromagnetic wave (i.e., a current or photovoltage effect can be observed).

The mathematical basis of the photon-drag effect arises from the first-order terms of the matrix element of the free-carrier–photon–phonon interaction when the matrix elements are expanded in terms of the wave vector of the photons.

The photon-drag effect was experimentally observed by Danishevakii *et al.*[4] and by Gibson *et al.*[5]

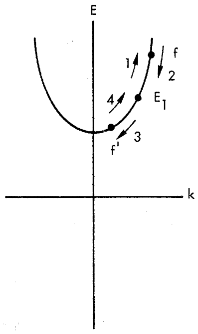

FIG. 1. Energy-band diagram showing the possible transitions that affect the distribution function of the electron at the energy state $E(k_i)=E_i$.

The theoretical basis was established by Grinberg[6] in germanium crystals using the model of electron–photon–acoustic-phonon interaction. The experimental results agreed quite well with the theory.

The purpose of this paper is to present the theory of the photon-drag effect in polar crystals based upon the Fröhlich model of interaction between the polar phonon and the electron. Because the universal relaxation time has no meaning for cases where the temperature is such that $kT < h\nu_p$, we will only treat the cases where $kT > h\nu_p$.[7,8]

In the calculations that follow, we will first find the change of the distribution function of the free carrier due to the electron-phonon-photon interaction and then, using the Boltzmann transport equation, we will determine the field generated by the photon-drag effect.

II. CALCULATION

The Hamiltonian for the interaction of the photon-electron-phonon system can be written as follows:

$$\mathcal{H}_T\psi=\left(-\frac{\nabla^2}{2m_0}+V(r)\right)\psi+\Big(\sum_k V_k a_k e^{i\vec{k}\cdot\vec{r}}+V_k^\dagger a_k^\dagger e^{-i\vec{k}\cdot\vec{r}}\Big)\psi+\sum_k \hbar\omega_p a_k^\dagger a_k\psi+\left(\frac{e}{m_0c}\vec{A}_R\cdot\vec{p}+\frac{e^2}{2m_0c}\vec{A}_R\cdot\vec{A}_R\right)\psi=\frac{\hbar}{i}\frac{\partial\psi}{\partial t}, \tag{1}$$

where the dagger indicates the Hermitian conjugate of the annihilation operator, $\vec{A}_R=\vec{A}(t,\vec{r})+\vec{A}^*(t,\vec{r})$ is the vector potential of the incident light, and

$$V_k=-\frac{i\hbar}{k}\left[\frac{2\pi\omega_p}{V}\frac{e^2}{\hbar}\left(\frac{1}{\epsilon_\infty}-\frac{1}{\epsilon_0}\right)\right]^{1/2}=-\frac{1}{k}a=af(k), \tag{2}$$

where ω_p is the frequency of the optical phonons and m_0 is the electron mass in free space.

From Eq. (1) we can calculate all the possible transitions which will affect the distribution function of the free carriers in the conduction bands.

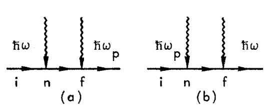

FIG. 2. Feynman diagram for (a) M_{if}^1 and (b) M_{if}^2.

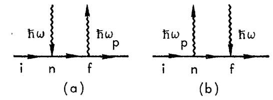

FIG. 3. Feynman diagram for (a) M_{if}^3 and (b) M_{if}^4.

Figure 1 shows the possible transitions which satisfy the conservation of energy $E_f=E_i+\hbar\omega\pm\hbar\omega_p$ (arrows "1" and "2") and $E_i=E_{f'}+\hbar\omega\pm\hbar\omega_p$ (arrows "3" and "4"). The Feynman diagrams (Figs. 2–9) show the possible alternatives in which an electron can absorb or emit a photon with the participation of a phonon. Arrow 1 of Fig. 1 represents the absorption of the photon by the electrons from an energy state E_i to E_f with participation of a phonon. Evaluating the matrix elements of this process using perturbation theory gives the following results:

$$M_{if}^1=\frac{af(k)(n_k)^{1/2}(\vec{\alpha}\cdot\hbar\vec{k}_i)\,\delta_{\vec{k}_f,\vec{k}+\vec{k}_i+\vec{q}}}{E(\vec{k}_i+\vec{q})-E(\vec{k}_i)-\hbar\omega}\left(\frac{eA}{mc}\right), \tag{3}$$

$$M_{if}^2=\frac{af(k)(n_k)^{1/2}\,\vec{\alpha}\cdot\hbar(\vec{k}_i+\vec{k})\,\delta_{\vec{k}_f(\vec{k}_i+\vec{k}+\vec{q})}}{E(\vec{k}_i+\vec{k})-E(k_f)-\hbar\omega}\left(\frac{eA}{mc}\right), \tag{4}$$

$$M_{if}^3\cong\frac{a^*f(k)(n_k+1)^{1/2}(\vec{\alpha}\cdot\hbar\vec{k}_i)\,\delta_{\vec{k}_f,\vec{k}_i+\vec{q}-\vec{k}}}{E(\vec{k}_i+\vec{q})-E(\vec{k}_i)-\hbar\omega}\left(\frac{eA}{mc}\right), \tag{5}$$

$$M_{if}^4\cong\frac{a^*f(k)(n_k+1)^{1/2}[\vec{\alpha}\cdot\hbar(\vec{k}_i-\vec{k})]\,\delta_{\vec{k}_f,\vec{q}+\vec{k}_i-\vec{k}}}{E(\vec{k}_i-\vec{k})-E(\vec{k}_f)+\hbar\omega}\left(\frac{eA}{mc}\right), \tag{6}$$

where $\vec{\alpha}$ is a unit polarization vector of the vector potential and A is the amplitude of the vector potential.

Arrow 2 of Fig. 1 represents the case where the electron makes a transition to the energy state E_i by the emission of a photon with simultaneous emission or absorption of a phonon. The matrix elements which represent these transitions are:

$$M_{if}^5=\frac{a^*f(k)(n_k+1)^{1/2}(\vec{\alpha}\cdot\hbar\vec{k}_f)\,\delta_{\vec{k}_i,\vec{k}_f-\vec{q}-\vec{k}}}{E(k_i+k)-E(\vec{k}_f)+\hbar\omega}\left(\frac{eA^*}{mc}\right), \tag{7}$$

$$M_{if}^6=\frac{a^*f(k)(n_k+1)^{1/2}[\vec{\alpha}\cdot\hbar(\vec{k}_i+\vec{q})]\,\delta_{\vec{k}_i,\vec{k}_f-\vec{q}-\vec{k}}}{E(\vec{k}_i+\vec{q})-E(\vec{k}_i)-\hbar\omega}\left(\frac{eA^*}{mc}\right), \tag{8}$$

$$M_{if}^7=\frac{af(k)(n_k)^{1/2}(\vec{\alpha}\cdot\hbar\vec{k}_f)\,\delta_{\vec{k}_i,\vec{k}_f-\vec{q}+\vec{k}}}{E(\vec{k}_f-\vec{q})-E(\vec{k}_f)+\hbar\omega}\left(\frac{eA^*}{mc}\right), \tag{9}$$

$$M_{if}^8=\frac{af(k)(n_k)^{1/2}\,\vec{\alpha}\cdot\hbar(\vec{k}_f+\vec{k})\,\delta_{\vec{k}_i,\vec{k}_f+\vec{k}-\vec{q}}}{E(\vec{k}_i+\vec{q})-E(\vec{k}_i)-\hbar\omega}\left(\frac{eA^*}{mc}\right). \tag{10}$$

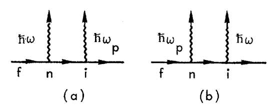

FIG. 4. Feynman diagram for (a) M_{if}^5 and (b) M_{if}^6.

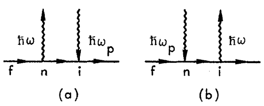

FIG. 5. Feynman diagram for (a) M_{if}^{7} and (b) M_{if}^{8}.

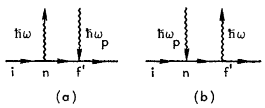

FIG. 7. Feynman diagram for (a) M_{if}^{11} and (b) M_{if}^{12}.

The matrix elements which represent the transition as indicated by arrow 3 of Fig. 1 are

$$M_{if}^{9}=\frac{a^{*}f(k)(n_k+1)^{1/2}(\vec{\alpha}\cdot\hbar\vec{k}_i)\delta_{\vec{k}_f,-\vec{q}-\vec{k}+\vec{k}_i}}{E(\vec{k}_i-\vec{q})-E(\vec{k}_i)+\hbar\omega}\left(\frac{eA^{*}}{mc}\right), \tag{11}$$

$$M_{if}^{10}=\frac{a^{*}f(k)(n_k+1)^{1/2}[\vec{\alpha}\cdot\hbar(\vec{k}_i-\vec{k})]\delta_{\vec{k}_f,\vec{k}_i-\vec{k}-\vec{q}}}{E(\vec{k}_i-\vec{k})-E(\vec{k}_f)-\hbar\omega}\left(\frac{eA^{*}}{mc}\right), \tag{12}$$

$$M_{if}^{11}=\frac{af(k)(n_k)^{1/2}(\vec{\alpha}\cdot\hbar\vec{k}_i)\delta_{\vec{k}_f,\vec{k}_i-\vec{q}+\vec{k}}}{E(\vec{k}_i-\vec{q})-E(\vec{k}_i)+\hbar\omega}\left(\frac{eA^{*}}{mc}\right), \tag{13}$$

$$M_{if}^{12}=\frac{af(k)(n_k)^{1/2}[\vec{\alpha}\cdot\hbar(\vec{k}_i+\vec{k})]\delta_{\vec{k}_f,\vec{k}_i+\vec{k}-\vec{q}}}{E(\vec{k}_f+\vec{q})-E(\vec{k}_f)-\hbar\omega}\left(\frac{eA^{*}}{mc}\right). \tag{14}$$

The matrix elements which represent the transition as indicated by arrow 4 of Fig. 1 are

$$M_{if}^{13}=\frac{a^{*}f(k)(n_k+1)^{1/2}(\vec{\alpha}\cdot\hbar\vec{k}_i)\delta_{\vec{k}_i,\vec{k}_f-\vec{k}+\vec{q}}}{E(\vec{k}_i-\vec{q})-E(\vec{k}_i)+\hbar\omega}\left(\frac{eA}{mc}\right), \tag{15}$$

$$M_{if}^{14}=\frac{a^{*}f(k)(n_k+1)^{1/2}(\vec{\alpha}\cdot\hbar\vec{k}_f)\delta_{\vec{k}_i,\vec{k}_f+\vec{q}-\vec{k}}}{E(\vec{k}_f+\vec{q})-E(\vec{k}_f)-\hbar\omega}\left(\frac{eA}{mc}\right), \tag{16}$$

$$M_{if}^{15}=\frac{af(k)(n_k)^{1/2}(\vec{\alpha}\cdot\hbar\vec{k}_f)\delta_{\vec{k}_i,\vec{k}_f+\vec{q}+\vec{k}}}{E(\vec{k}_f+\vec{q})-E(\vec{k}_f)-\hbar\omega}\left(\frac{eA}{mc}\right), \tag{17}$$

$$M_{if}^{16}=\frac{af(k)(n_k)^{1/2}[\vec{\alpha}\cdot\hbar(\vec{k}_f+\vec{k})]\delta_{\vec{k}_i,\vec{k}+\vec{q}+\vec{k}}}{E(\vec{k}_i-\vec{q})-E(\vec{k}_i)+\hbar\omega}\left(\frac{eA}{mc}\right), \tag{18}$$

where $\vec{q}$ is the wave vector of the photon.

Using the matrix elements given in Eqs. (3)–(18) and assigning the factor f or $1-f$ (where f is the probability distribution function) as appropriate for each transition to accommodate the Pauli exclusion principle, we obtain the following partial derivative of the distribution function due to the interaction of the photon, the phonon, and the electron:

$$\left.\frac{\partial f}{\partial t}\right|_{p}=\left(\frac{2\pi}{\hbar}\right)\sum_{k_f}\sum_{k}\left(\sum_{i=i}^{4}\frac{\partial f_i}{\partial t}\right), \tag{19}$$

$$\frac{\partial f_1}{\partial t}=\{f(k_f)[1-f(k_i)]\,|M_{if}^{5}+M_{if}^{6}|^{2}-f(k_i)[1-f(k_f)]\,|M_{if}^{1}+M_{if}^{2}|^{2}\}\delta(E_f-E_i-\hbar\omega_p-\hbar\omega), \tag{20}$$

$$\frac{\partial f_2}{\partial t}=\{f(k_f)[1-f(k_i)]\,|M_{if}^{7}+M_{if}^{8}|^{2}-f(k_i)[1-f(k_f)]\,|M_{if}^{3}+M_{if}^{4}|^{2}\}\delta(E_f-E_i-\hbar\omega+\hbar\omega_p), \tag{21}$$

$$\frac{\partial f_3}{\partial t}=\{f(k_{f'})[1-f(k_i)]\,|M_{if'}^{13}+M_{if'}^{14}|^{2}-f(k_i)[1-f(k_{f'})]\,|M_{if'}^{11}+M_{if'}^{12}|^{2}\}\delta(E_i-E_{f'}-\hbar\omega+\hbar\omega_p), \tag{22}$$

$$\frac{\partial f_4}{\partial t}=\{f(k_{f'})[1-f(k_i)]\,|M_{if}^{15}+M_{if'}^{16}|^{2}-f(k_i)[1-f(k_{f'})]\,|M_{if'}^{9}+M_{if'}^{10}|^{2}\}\delta(E_i-E_{f'}-\hbar\omega-\hbar\omega_p). \tag{23}$$

After carrying out the summation for $\vec{k}$ and changing the summation on $\vec{k}_f$ to an integral, we obtain the following results:

$$\left.\frac{\partial f}{\partial t}\right|=\frac{2\pi}{\hbar}\frac{V}{(2\pi)^{3}}\{f(E_{k_i}+\hbar\omega+\hbar\omega_p)[1-f(E_{k_i})](n_k+1)-f(E_{k_i})[1-f(E_{k_i}+\hbar\omega+\hbar\omega_p)]n_k\}\left|a\left(\frac{eA}{mc}\right)\right|^{2}$$

$$\times\int d\vec{k}_f\,\delta(E_f-E_i-\hbar\omega-\hbar\omega_p)M_1+\frac{2\pi}{\hbar}\frac{V}{(2\pi)^{3}}\{f(E_{k_i}+\hbar\omega-\hbar\omega_p)[1-f(E_{k_i})]n_k-f(E_{k_i})[1-f(E_{k_i}+\hbar\omega-\hbar\omega_p)](n_k+1)\}$$

$$\times\left|a\left(\frac{eA}{mc}\right)\right|^{2}\int d\vec{k}_f\,\delta(E_f-E_i-\hbar\omega+\hbar\omega_p)M_2+\frac{2\pi}{\hbar}\frac{V}{2(\pi)^{3}}$$

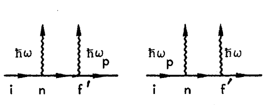

FIG. 6. Feynman diagram for (a) M_{if}^{9} and (b) M_{if}^{10}.

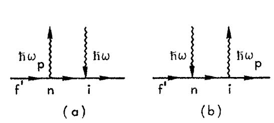

FIG. 8. Feynman diagram for (a) M_{if}^{13} and (b) M_{if}^{14}.

$$\times\{f(E_{k_i}-\hbar\omega+\hbar\omega_p)[1-f(E_{k_i})](n_k+1)-f(E_{k_i})[1-f(E_{k_i}-\hbar\omega+\hbar\omega_p)]n_k\}$$

$$\times\left|a\left(\frac{eA}{mc}\right)\right|^2\int d\vec{k}_f M_3\delta(E_i-E_f-\hbar\omega+\hbar\omega_p)+\frac{2\pi}{\hbar}\frac{V}{(2\pi)^3}\{f(E_{k_i}-\hbar\omega-\hbar\omega_p)\,[1-f(E_{k_i})]n_k$$

$$-f(E_{k_i})[1-f(E_{k_i}-\hbar\omega-\hbar\omega_p)](n_k+1)\}\left|a\left(\frac{eA}{mc}\right)\right|^2\int d\vec{k}_f M_4\delta(E_i-E_f-\hbar\omega-\hbar\omega_p)\ , \qquad (24)$$

where

$$n_k=1/(e^{\hbar\omega_p/kT}-1)$$

and

$$M_1=M_2=\left|\left(\frac{1}{|\vec{k}_i+\vec{q}-\vec{k}_f|}\right)\left(\frac{\vec{\alpha}\cdot\hbar\vec{k}_i}{E(\vec{k}_i+\vec{q})-E(\vec{k}_i)-\hbar\omega}+\frac{\vec{\alpha}\cdot\hbar\vec{k}_f}{E(\vec{k}_f-\vec{q})-E(\vec{k}_f)+\hbar\omega}\right)\right|^2\ , \qquad (25)$$

$$M_3=M_4=\left|\frac{1}{|\vec{k}_f+\vec{q}-\vec{k}_i|}\left(\frac{\vec{\alpha}\cdot\hbar\vec{k}_i}{E(\vec{k}_i-\vec{q})-E(\vec{k}_i)+\hbar\omega}+\frac{\vec{\alpha}\cdot\hbar\vec{k}_f}{E(\vec{k}_f+\vec{q})-E(\vec{k}_f)-\hbar\omega}\right)\right|^2\ . \qquad (26)$$

Because the wave vector of the light, $\vec{q}$, is small when compared to the average momentum of the electrons, we can expand M_1, M_2, M_3, and M_4 in terms of $\vec{q}$ in a series and retain only the zero- and first-order terms in the expansion. These are

$$M_1=M_2=\frac{1}{|\vec{k}_f-\vec{k}_i|^2}\left(\frac{1}{\hbar\omega}\right)^2[\vec{\alpha}\cdot\hbar(\vec{k}_f-\vec{k}_i)]^2+\frac{1}{|k_i-k_f|^2}\left(\frac{1}{\hbar\omega}\right)^2$$

$$\times\frac{2\hbar^2}{m\hbar\omega}[\vec{\alpha}\cdot\hbar(\vec{k}_f-\vec{k}_i)][(\vec{\alpha}\cdot\hbar\vec{k}_f)(\vec{q}\cdot\vec{k}_f)-(\vec{\alpha}\cdot\hbar\vec{k}_i)(\vec{q}\cdot\vec{k}_i)]+\left(\frac{1}{\hbar\omega}\right)^2\frac{2\vec{q}\cdot\hbar(\vec{k}_f-\vec{k}_i)}{|\vec{k}_f-\vec{k}_i|^4}[\vec{\alpha}\cdot\hbar(\vec{k}_f-\vec{k}_i)]^2\ , \qquad (27)$$

$$M_3=M_4=\frac{1}{|\vec{k}_f-\vec{k}_i|^2}\left(\frac{1}{\hbar\omega}\right)^2[\vec{\alpha}\cdot\hbar(\vec{k}_f-\vec{k}_i)]^2+\frac{1}{|\vec{k}_i-\vec{k}_f|^2}\left(\frac{1}{\hbar\omega}\right)^2\frac{2\hbar^2}{m\hbar\omega}$$

$$\times[\vec{\alpha}\cdot\hbar(\vec{k}_f-\vec{k}_i)]\,[(\vec{\alpha}\cdot\hbar\,\vec{k}_f)\,(\vec{q}\cdot\vec{k}_f)-(\vec{\alpha}\cdot\hbar\vec{k}_i)\,(\vec{q}\cdot\vec{k}_i)]-\left(\frac{1}{\hbar\omega}\right)^2\frac{2\,\vec{q}\cdot(\vec{k}_f-\vec{k}_i)}{|\vec{k}_f-\vec{k}_i|^4}[\vec{\alpha}\cdot\hbar(\vec{k}_f-\vec{k}_i)]^2\ . \qquad (28)$$

So that the photon-drag effect will not be influenced by the optical absorption of the optical phonon, we assume that the excitation energy of the photon is much higher than that of the optical phonon (i.e., $h\nu\gg h\nu_p$). Using this assumption, the approximation given in Eqs. (27) and (28) for matrix elements, and the coordinate system of Fig. 10, we obtain the integrals given in Eq. (24) as follows:

$$I_{\bar{i}}=\int M_{\bar{i}}\,\delta(E_f-E_i-\hbar\omega\pm\hbar\omega_p)\,d\vec{k}_f$$

$$\cong\left(\frac{2m}{\hbar^2}\right)^2\frac{4\pi q\hbar^2}{(\hbar\omega)^2}\,\frac{\hbar^2}{m}\,(E_i)^{1/2}(E_i+\hbar\omega)^{1/2}\left\{\frac{1}{3\hbar\omega}\left[2+\frac{1}{5}\left(\frac{E_i}{E_i+\hbar\omega}\right)^2\right]-\frac{1}{2(E_i+\hbar\omega)}\left[\frac{1}{3}+\left(\frac{2E_i}{E_i+\hbar\omega}\right)^2\right]\right\}$$

$$\times(\cos^2\theta)\,(\sin\theta)(\sin\phi)\ \ (\bar{i}=1\text{ or }2)\ , \qquad (29)$$

$$I_j=\int M_j\,\delta(E_i-E_f-\hbar\omega\pm\hbar\omega_p)d\vec{k}_f$$

$$\cong\left(\frac{2m}{\hbar^2}\right)^2\frac{4\pi q\hbar^2}{(\hbar\omega)^2}\,\frac{\hbar^2}{m}\,(E_i-\hbar\omega)^{1/2}(E_i)^{1/2}\left\{\frac{1}{\hbar\omega}\left[1-\frac{1}{3}\left(\frac{E_i-\hbar\omega}{E_i}\right)-\frac{2}{15}\left(\frac{E_i-\hbar\omega}{E_i}\right)^2\right]+\frac{1}{2E_i}\left[1-\frac{1}{3}\left(\frac{E_i-\hbar\omega}{E_i}\right)^{3/2}\right]\right\}$$

$$\times\cos^2\theta\,\sin\theta\,\sin\phi\quad(j=3,4)\ . \qquad (30)$$

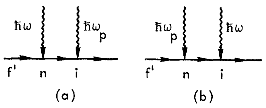

FIG. 9. Feynman diagram for (a) M_{if}^{15} and (b) M_{if}^{16}.

In a polar crystal, the definition of relaxation time has no meaning. However, as pointed out by Howarth and Sondheimer[7] and Ehrenreich,[8] when the temperature of the crystal is such that $\hbar\omega_p < kT$, universal relaxation time may be defined as

$$\tau(E_i) = (\hbar\omega_p)\left(\frac{\hbar\omega_p}{2m}\right)^{1/2} \frac{1}{n_\omega}\left(\frac{E_i}{\hbar\omega_p}\right)^r \times\left(\frac{1}{e^2\,\omega_p^2(1/\epsilon_\infty - 1/\epsilon_0)}\right) , \qquad (31)$$

where the value of r satisfies $1/2 \geq r \geq 0$. We can now write the Boltzmann equation for the photon-drag effect as follows[6]:

$$\frac{e}{\hbar}\left[\vec{\mathrm{E}}\cdot\vec{\nabla}_k f_0(E_k)\right] - \left(\frac{f-f_0}{\tau}\right) + \frac{\partial f_p}{\partial t} = 0 , \qquad (32)$$

where the $\partial f_p/\partial t$ is that given in Eq. (24).

We assume the distribution function f does not deviate very much from the equilibrium distribution function f_0 by putting $f = f_0$ in Eq. (24). This assumption was found to be a good approximation in previous work.[6,9] Using this assumption together with Eq. (24), we obtain the following expression for the current:

$$j \cong -\left(\frac{1}{(2\pi)^3}\right)^2 Ve\,\frac{\hbar}{m}\,\frac{1}{2}\left(\frac{2m}{\hbar^2}\right)^2 \frac{2\pi}{\hbar}\int E_i\,dE_i\,(\sin^2\theta)(\sin\phi)\,d\theta\,d\phi\;\tau(E_i)(-1)f_0(E_i)\left|\frac{eA}{mc}\right|^2(2n_k+1)|a|^2 I_1$$

$$+(-1)\left(\frac{1}{(2\pi)^3}\right)^2\left(\frac{Ve\hbar}{m}\right)\frac{2\pi}{\hbar}\,\frac{1}{2}\left(\frac{2m}{\hbar^2}\right)^2\int E_i\,dE_i\,(\sin^2\theta)(\sin\phi)\,d\theta\,d\phi\;\tau(E_i)f(E_i-\hbar\omega)(2n_k+1)\left|\frac{eA}{mc}\right|^2|a|^2 I_3$$

$$-e\,\frac{\hbar}{m}\,\frac{e}{\hbar}\,\frac{1}{(2\pi)^3}\,\frac{1}{2}\left(\frac{2m}{\hbar^2}\right)^2\int \tau(E_i)\,E_i\,dE_i\,\vec{\mathrm{E}}\cdot\vec{\nabla}_k f_0\,(\sin\theta)^2(\sin\phi)\,d\theta\,d\phi , \qquad (33)$$

where I_1 and I_3 are those given in (29) and (30),

$$|A|^2 = 2\pi c I/\epsilon_\infty^{1/2}\,\omega^2 ,$$

I is the intensity of the light, and $\vec{\mathrm{E}}$ is the electric field in the crystal.

Now if we put $j = 0$, we obtain the electric field E generated by the photon-drag effect at the distance y in the crystal:

$$E_y \cong \frac{-\frac{2^6}{15}\,e^3\,(q\pi^2/mc)\,(I\hbar^2/\epsilon^{1/2})\,[\hbar\omega_p/(\hbar\omega)^4]\,(1/\epsilon_\infty - 1/\epsilon_0)\,(2n_k+1)}{\int_0^\infty \tau(E_i)\,E_i\,dE_i\,\nabla_{k_y} f_0\sin^2\theta\,\sin\phi\,d\theta\,d\phi}\int_0^\infty dE_i\,[(E_i+\hbar\omega)\,E_i]^{1/2} f_0$$

$$\times\left\{(E_i+\hbar\omega)\,\tau(E_i+\hbar\omega)\left[\frac{1}{\hbar\omega}\left(1-\frac{1}{3}\,\frac{E_i}{E_i+\hbar\omega}\right)-\frac{2}{15}\left(\frac{E_i}{E_i+\hbar\omega}\right)^2\left(\frac{1}{\hbar\omega}\right)\right]+(E_i+\hbar\omega)\tau(E_i+\hbar\omega)\left(\frac{1}{2(E_i+\hbar\omega)}\right.\right.$$

$$\left.\left.\times\left[1-\frac{1}{3}\left(\frac{E_i}{E_i+\hbar\omega}\right)^{3/2}\right]-E_i\,\tau(E_i)\,\frac{1}{3}\,\frac{1}{\hbar\omega}\left[2+\frac{1}{5}\left(\frac{E}{E_i+\hbar\omega}\right)^2\right]+E_i\,\tau(E_i)\right)\frac{1}{2(E_i+\hbar\omega)}\left[\frac{1}{3}+\left(\frac{E_i}{E_i+\hbar\omega}\right)^2\right]\right\} = \bar{K} I . \qquad (34)$$

Let us now evaluate Eq. (34) for some special values of r and for a nondegenerated semiconductor.

Case 1. For $r = \frac{1}{2}$, Eq. (34) takes the form

$$E_y \cong \tfrac{8}{5}\pi\,\frac{n_0\,e^3}{\sigma}\left(\frac{\hbar\omega_p}{\hbar\omega}\right)^3\frac{Iq}{c\omega_p^3}\left(\frac{1}{m^2\,\epsilon_\infty^{1/2}}\right)(2n_\omega+1) \times\left(1+\frac{2kT}{\hbar\omega}\right)\left(\frac{\hbar\omega_p}{kT}\right). \qquad (35)$$

Case 2. For $r = 0$, Eq. (34) becomes

$$E_y = \frac{8\sqrt{2}}{5}\,\frac{n_0\,e^3}{\sigma}\,\frac{1}{m^2\,\epsilon_\infty^{1/2}}\,\frac{q\pi}{c}\,\frac{I\hbar^3}{(\hbar\omega_p)^2}\left(\frac{\hbar\omega_p}{\hbar\omega}\right)^{5/2} \times\left(\frac{1}{\hbar\omega}\right)\left(1+\frac{3}{4}\,\frac{kT}{\hbar\omega}\right)\left(\frac{2n_\omega+1}{n_\omega}\right) , \qquad (36)$$

where σ is the conductivity of the crystal, $n_\omega = n_k$,[10] and n_0 is the free-carrier density.

According to the work of Howarth and Sondheimer[7] and Ehrenreich,[8] Eqs. (35) and (36) should be applicable (or at least give an approximation) for the case in which $kT > h\nu_p$ and in which $kT \cong h\nu_p$,

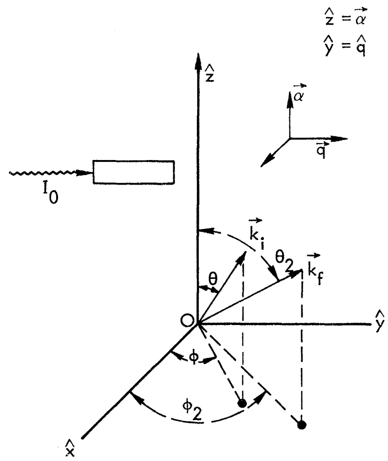

FIG. 10. Coordinate system used for the calculation.

respectively.

As an order-of-magnitude calculation, we apply Eq. (35) to the CdS crystal. Using $m = 0.2m_0$,[11] $I = 1\ \text{MW/cm}^2$, $\epsilon_\infty = 9.25$, $kT = 0.05$ eV, $h\nu_p = 0.038$ eV,[11] and $h\nu = 0.12$ eV (10.6-μ CO_2 laser), we find the electric field is

$$E_y = 0.1\ \text{V/cm}.$$

For the case in which $kT \cong \hbar\nu_p$, we use Eq. (36) and find that the electric field is

$$E_y = 0.2\ \text{V/cm}\ .$$

In investigating the photon-drag effect, what we usually measure is the potential difference across the crystal. This potential difference is obtained by letting $I = I_0(1-R)e^{-\alpha y}$ in Eq. (34), where α is the absorption coefficient and R is the reflection coefficient, and then integrating the resulting equation to obtain the potential across the crystal:

$$V = -(1/\alpha)(1-R)I_0\overline{K}\ . \tag{37}$$

It is interesting to note that Eq. (37) has the same dependence upon the carrier density as that obtained by Gibson *et al.*[5] for germanium crystals.

In Eq. (34) we let $I = I_0 e^{-\alpha y}$ and then integrate to obtain Eq. (37). We were able to do this because the usual length of the crystals used for this study is a few centimeters. As a result, we can theoretically divide the crystal into many sections (say n sections), each of which retains the characteristics of the whole crystal. Now in the case of the photon–free-carrier–phonon interaction, the decrease of light intensity is very slow with respect to the distance traveled in the crystal. Consequently, when evaluating the matrix elements for each section, we can consider the amplitude of the vector potential a constant. We account for the change in vector potential as we go from one section to another by letting $|A|_j^2$ be proportional to $I_0 e^{-\alpha y j}$, where j designates the jth section of the crystal. It then follows that the electric field can be written as $E_{yj} = \overline{K} I_j$. Hence, to obtain the total potential across the crystal, we simply sum up all the contributions from all the sections and obtain

$$V = -\sum_{j=1}^{n} E_{yj}\,\Delta y\ . \tag{38}$$

Or, in the limiting case, we may write as an integral

$$V = -\int_0^L E_y\,dy\ . \tag{39}$$

III. DISCUSSION AND CONCLUSIONS

In deriving the matrix elements M_{if}^1 to M_{if}^{16}, we have intentionally left out the exact form of $\alpha f(k)$. As a result, these matrix elements can be transformed to the case of the electron–photon–acoustic-phonon interaction by making a proper substitution for $\alpha f(k)$. Therefore, the theory presented is much more general than we indicated earlier.

Although the derivation of Eqs. (35) and (36) was made for crystals above room temperatures, it may also be used for order-of-magnitude calculations for some semiconductor crystals at room temperature. The reason for this is that when a high-intensity laser beam (with power such as MW/cm^2) is incident upon the crystal, the temperature inside the crystal will rise into the region where Eq. (36) is valid.

The numerical calculation for the CdS crystal shows that we should be able to observe the photon-drag effect in this crystal. Because the polar coupling coefficient and $h\nu_p$ are numerically very close for many crystals (such as GaAs, InSb, etc.), we suspect that the polar phonon also plays an important role in the photon-drag phenomena in these crystals.[10]

It is also interesting to note that the value of the longitudinal phonon energy ($\hbar\omega_p$) of many polar crystals is smaller than kT at room temperature. Therefore, the theory presented here is valid for those crystals at room temperature.

---

*Work performed under the auspices of the U. S. Atomic Energy Commission.

[1]N. Bloembergen, Proc. IEEE 51, 124 (1963).

[2]A. Gold, in *Quantum Optics*; *Enrico Fermi International School of Physics*, *Course XLII*, edited by R. J. Glauber (Academic, New York, 1969).

[3]S. L. McCall and E. L. Hahn, Phys. Rev. 183, 457 (1969).

[4]A. M. Danishevskii, A. A. Kastal'skii, S. M. Ryvkin, and I. D. Varoshetskii, Zh. Eksperim. i Teor. Fiz. 58, 544 (1970) [Sov. Phys. JETP 31, 292 (1970)].

[5]A. F. Gibson, M. F. Kimmitt, and A. C. Walker,

Appl. Phys. Letters 17, 75 (1970).
[6]A. A. Grinberg, Zh. Eksperim. i Teor. Fiz. 58, 989 (1970) [Sov. Phys. JETP 31, 531 (1970)].
[7]D. J. Howarth and E. H. Sondheimer, Proc. Roy. Soc. (London) A219, 53 (1953).
[8]H. Ehrenreich, J. Appl. Phys. 32, 2155 (1961).
[9]A. S. Baltenkov, N. A. Brynskikh, V. B. Gilerson, and N. I. Kramer, Fiz. i Tekh. Poluprovodnikov 4, 1851 (1970) [Sov. Phys. Semicond. 4, 1589 (1971)].
[10]F. C. Brown, in *Polarons and Excitons*, edited by C. G. Kuper and G. D. Whitfield (Plenum, New York, 1962).
[11]J. J. Hopfield and D. G. Thomas, Phys. Rev. 122, 35 (1961).

PHYSICAL REVIEW B VOLUME 6, NUMBER 6 15 SEPTEMBER 1972

Pressure-Induced Electronic Collapse and Structural Changes in Rare-Earth Monochalcogenides

A. Chatterjee and A. K. Singh
Materials Science Division, National Aeronautical Laboratory, Bangalore 17, India

and

A. Jayaraman*
Bell Telephone Laboratories, Murray Hill, New Jersey 07974
(Received 2 May 1972)

The compressibilities of the monotellurides of Pr, Sm, Eu, Tm, and Yb and the monoselenide and sulfide of Sm have been investigated to ~300 kbar using high-pressure x-ray-diffraction techniques. SmTe, SmSe, TmTe, and YbTe show abnormal volume changes in the 20–50-, 15–40-, 15–30-, and 150–200-kbar regions of pressure, respectively. SmS shows an abrupt decrease in volume at 6.5 kbar. Since there is no change in structure, the anomalously large volume changes have been explained on the basis of a pressure-induced $4f$-$5d$ electronic collapse which involves a change in the valence state of the rare-earth ion from 2^+ towards the 3^+ state. The results of high-pressure x-ray studies on Sm chalcogenides are consistent with the conclusions drawn in the earlier work from high-pressure resistivity measurements. PrTe, SmTe, and EuTe exhibit a phase transition from NaCl-type to CsCl-type structure at pressures of about 90 ± 10, 110 ± 10, and 110 ± 10 kbar, respectively. It appears that a pressure-induced NaCl-to-CsCl transition may be commonly encountered in rare-earth monochalcogenides.

INTRODUCTION

Rare-earth monochalcogenides have attracted much attention in recent years because of their interesting magnetic and electrical properties. They crystallize in the NaCl-type structure[1] and are semiconducting if the rare-earth ion is in the divalent state and metallic if trivalent.[2,3] Recent high-pressure resistivity studies[4–6] on Sm chalcogenides and TmTe revealed that these undergo a pressure-induced semiconductor-metal transition; the transition is found to be continuous in the case of SmTe, SmSe, and TmTe, while discontinuous in the case of SmS. This phenomenon was interpreted as due to the promotion of a $4f$ electron of the rare-earth ion into the $5d$ conduction-band states, as the energy separation between the localized $4f$ electronic state and the latter decreased with pressure. Such an electronic transition involves a change of the valence state of the rare-earth ion from divalent to a higher valence state tending towards trivalency. Since the ionic radius of the trivalent ion is substantially smaller than that of the corresponding divalent ion, the occurrence of $4f$-$5d$-electron promotion should be reflected in the pressure-volume behavior, and hence the pressure-volume relationship should provide conclusive evidence for $4f$-$5d$-electron promotion. Therefore, we undertook a high-pressure x-ray study of a number of rare-earth monochalcogenides of interest in this connection. The results will be presented and discussed in this paper.

EXPERIMENTS AND RESULTS

The pressure-volume data up to nearly 300 kbar were obtained from lattice-parameter measurements, using a diamond-anvil high-pressure x-ray camera.[7] In the pressure range 1–50 kbar, measurements were also made using the McWhan-Bond high-pressure camera.[8] Pressure was estimated using NaCl or Ag as an internal standard. At pressures above 50 kbar, the diffraction lines from NaCl became too weak when using the diamon-anvil camera, due to the extrusion of the salt from the center of the anvil. However, silver proved quite satisfactory at higher pressures. The